

## Spectral characteristics in resonators with fractal boundaries

Yutaka Hobiki, Kousuke Yakubo, and Tsuneyoshi Nakayama  
*Department of Applied Physics, Hokkaido University, Sapporo 060, Japan*  
 (Received 14 February 1996)

Vibrations of drums with self-similar (fractal) boundaries are investigated in terms of large-scale simulations, for elucidating the characteristics of their spectral densities of states. It is found that the integrated density of states  $\Delta I(\omega)$  is proportional to  $\omega^{D_f}$  ( $D_f$  the fractal dimension of the boundary) in the frequency regime higher than a characteristic frequency  $\omega_c$  with oscillating but small amplitude. The frequency  $\omega_c$  is related to the length scale characterizing the fractal boundary. We show that there exist edge modes localized near the fractal boundary under the stress-free boundary condition (Neumann condition), which vibrate at both ends of the drum with antiphase. [S1063-651X(96)06808-0]

PACS number(s): 03.40.Kf, 63.50.+x, 68.35.Ja, 71.55.Jv

### I. INTRODUCTION

The concept of fractals is crucial for describing dynamic as well as static properties of complex geometries [1–4]. There are two types of fractal systems showing peculiar vibrational properties, mass fractals and structures with fractal perimeters. The first mainly concerns harmonic vibrations called fractons [5]. The second one is related to vibrations excited in systems with fractal perimeters [6]. These systems, so-called fractal drums, have significant physical implications, i.e., water waves in a lake (seiches), acoustic waves in a concert hall with irregular walls, vibrations of fluid in porous media, and oscillations of the whole earth. The asymptotic properties of the integrated densities of states (IDOS) of fractal drums, in the high frequency limit, have been discussed from mathematical points of view [7–10]. Thus fractal drums have attracted great interest of both physicists and mathematicians. A conjecture [7] was given that the fractal dimension  $D_f$  of the perimeter is relevant to the IDOS of the drum. This is called the Berry-Lapidus (BL) conjecture. The BL conjecture has been numerically studied for the first time by Sapoval *et al.* [6,11–13] via calculations of the IDOS of the fractal drum with the Koch-curve boundary (Koch drum) at the second generation with  $D_f=1.5$ . They used a mapping relation between the Helmholtz and the diffusion equations. They calculated eigenfrequencies (and their distribution) and the corresponding eigenfunctions of the Koch drum. Although their method employed can find accurate eigenfrequencies and the eigenstates, only a small part of lower eigenfrequencies and their eigenstates were obtained due to the limitation of the CPU time. In fact, they have calculated only 3% of all eigenmodes. In order to obtain correct insight into the characteristics of the IDOS, the sufficient generation of a fractal drum reflecting the fractality of the boundary and the calculation of the IDOS at high enough eigenfrequencies are necessary.

Hobiki, Yakubo, and Nakayama [14] have recently studied the IDOS's of Koch drums at the third and fifth generations by employing a simple but powerful and accurate numerical method. They have calculated the IDOS in two orders of the frequency range, and found that the IDOS  $\Delta I(\omega)$  is proportional to  $\omega^{D_f}$  with  $D_f=1.5$  in the frequency regime higher than a characteristic frequency  $\omega_c$ . This result is valid for drums with the Koch-curve boundary. The spec-

tral distribution is sensitive to the shape of the boundary. Whether the BL conjecture holds for other shaped drums has not yet been clarified.

The purpose of this paper is to investigate the characteristics of the IDOS of drums other than the Koch drum with  $D_f=1.5$  via large-scale simulations. We take two types of fractal drums at high generations. It will be shown that the IDOS's  $\Delta I(\omega)$  are proportional to  $\omega^{D_f}$  ( $D_f$  the fractal dimension) in the frequency regime higher than a characteristic frequency  $\omega_c$  related to the length scale characterizing the fractal boundary with oscillating but small amplitude.

The organization of this paper is as follows: Sec. II describes the basic concept of the BL conjecture related to vibrational properties of fractal drums. In Sec. III, the applicability of the conjecture for discretized lattice systems is discussed. We argue in detail this point by illustrating a square drum (0th generation), namely, about the Weyl-Seeley-Pham [15–17] asymptotic formula. The comparison of the exact expression for the IDOS of this system with the computed result will convince us to use the formula of Eq. (8) for investigating the BL conjecture. In Sec. IV, we outline our numerical method, called the forced oscillator method, which is employed to calculate the densities of states and mode patterns. The method is quite powerful to treat eigenvalue problems of very large matrices, by mapping them onto those of lattice systems. The numerical results are given in Sec. V. Section VI gives summary and discussions.

### II. ASYMPTOTIC FORMULAS FOR THE SPECTRAL DISTRIBUTION OF DRUMS WITH SMOOTH AND FRACTAL PERIMETERS

We consider, at first, vibrations of drums with fixed boundary condition (Dirichlet condition). Let  $R$  be an arbitrary shaped bounded region. The starting equation describing vibrations of drums is expressed by the Helmholtz equation,

$$(\Delta + \omega^2)u(\mathbf{r}) = 0 \quad \text{in } R, \quad (1)$$

where  $\omega$  is the eigenfrequency (or  $\omega^2$  the eigenvalue),  $\Delta$  denotes the Laplacian, and  $u(\mathbf{r})$  is the scalar displacement.

The Helmholtz equation (1) appears in various fields of physics, to describe not only propagations of electromagnetic and acoustic waves, but also energy spectra of electronic systems since Eq. (1) is equivalent to the Schrödinger equation. Eigenfrequencies consist of an infinite sequence of positive quantities. The lowest frequency  $\omega_1$  is called the fundamental tone and higher frequencies are overtones of the drum. The integrated density of states (IDOS) represents the number of eigenfrequencies of Eq. (1) up to  $\omega$ , which is given by

$$I_{\text{fix}}(\omega) = \int_0^\omega D(\omega') d\omega'. \quad (2)$$

The density of states is defined by  $D(\omega) = \sum_\lambda \delta(\omega - \omega_\lambda)$ , where  $\delta(x)$  is the Dirac delta function and  $\omega_\lambda$  the eigenfrequency. The suffix ‘‘fix’’ of Eq. (2) represents the IDOS under the fixed boundary condition (Dirichlet condition).

Seeley [16] and Pham [17] have obtained, by extending the Weyl’s asymptotic formula [15], the following asymptotic form of the IDOS for drums with the smooth boundary in the high frequency limit,

$$I_{\text{fix}}(\omega) = \frac{S}{4\pi} \omega^2 - B\omega + o(\omega) \quad (\omega \rightarrow \infty), \quad (3)$$

where  $S$  is the area of the drum and  $B$  a positive constant depending on a shape of the drum.  $o(\omega)$  denotes the Landau symbol. We call this the Weyl-Seeley-Pham (WSP) asymptotic formula. The first term of the right-hand side of Eq. (3) is the IDOS for a drum with the stress-free boundary (Neumann condition) in the high frequency limit. The second term is due to the vanishing degree of freedom by imposing the fixed boundary condition (Dirichlet condition). This term depends on the shape of the boundary and should be proportional to  $\omega$  for a one-dimensional (1D) and smooth perimeter.

The WSP asymptotic formula Eq. (3) assumes the smooth boundary. However, there are many drums and resonators possessing irregular and structurally disordered boundaries. Berry [7] and Lapidus [8–10] have extended the formula Eq. (3) to the case with a fractal boundary whose fractal dimension is expressed by  $D_f$ . Berry [7] has conjectured that the IDOS  $I_{\text{fix}}(\omega)$  of a fractal drum with the fixed boundary (Dirichlet) condition should have the following frequency dependence in the high frequency limit:

$$I_{\text{fix}}(\omega) = \frac{S}{4\pi} \omega^2 - B_f \omega^{D_f} + o(\omega^{D_f}) \quad (\omega \rightarrow \infty), \quad (4)$$

where  $S$  is the area of the drum and  $B_f$  a positive constant depending on the shape of the drum. This expression is called the Berry-Lapidus (BL) conjecture. The BL conjecture is based on the following assumptions: Vibrational modes of a drum with the stress-free boundary (Neumann) condition can be separated into the inside and the boundary parts, and vibrational modes related to the boundary have the linear dispersion relation. Quite recently, Levitin and Vassiliev [18] and Fleckinger, Levitin, and Vassiliev [19] have pointed out that the factor  $B_f$  is an oscillating function of frequency  $\omega$  but with a small amplitude. This will be argued in Sec. V in connection with our numerical results.

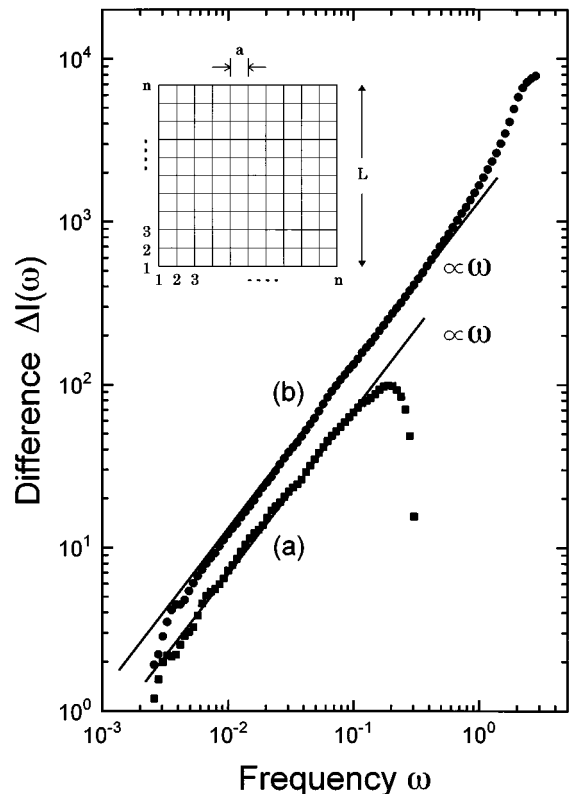


FIG. 1. The difference  $\Delta I(\omega)$  for the square drum with  $n=2000$  as a function of frequency  $\omega$ . The symbol  $n$  is the number of grid points at a side  $L$  of the square drum. Schematic illustration of the discretized square drum is given in the inset. We use the system of units  $m=1$ ,  $K=1$ , and  $a=1$ . The results given in (a) and (b) are obtained by using Eqs. (7) and (8), respectively. The difference  $\Delta I(\omega)$  in (b) is proportional to  $\omega$  even in the higher frequency regime compared with the case of (a).

### III. THE CONJECTURE FOR LATTICE SYSTEMS

Equations (3) and (4) assume that the drum consists of a continuum medium. We need to discretize the continuum drum to a lattice (or grid) system for real space numerical investigation. For this, Eqs. (3) and (4) are inapplicable directly because the discretized drum possesses a characteristic length, namely, a grid spacing  $a$ . This length scale becomes relevant in the high frequency limit. At first, we extend Eqs. (3) and (4) for discretized systems. The validity of this modification will be demonstrated by calculating numerically the IDOS for a discretized square drum, for which we have the rigorous dispersion relation.

Let us consider a simple square drum. The side length of the square drum is taken to be  $L$  (see the inset of Fig. 1), for which the dimension of the boundary becomes  $D_f=1$ . The dispersion relation of the discretized square drum obeys the following form:

$$\omega^2 = 4(K/m) \sum_{\alpha=x,y} \sin^2(k_\alpha a/2), \quad (5)$$

where  $m$  is a mass of a lattice point,  $K$  a spring constant, and  $k_\alpha$  the wave number along the  $\alpha$  direction. Hereafter, we use

the system of units  $m=1$ ,  $K=1$ , and  $a=1$  without loss of generality. Under the *fixed* boundary condition, the wave numbers  $k_\alpha$  are given by

$$k_\alpha = \frac{p\pi}{n-1}; \quad \text{for } p=1,2,\dots,n-2, \quad (6)$$

where  $n$  is the number of grid points on the side, i.e.,  $L=(n-1)a$  (see the inset of Fig. 1). Eigenfrequencies  $\omega$  are obtained by substituting the wave numbers  $k_\alpha$  given by Eq. (6) into Eq. (5), and the IDOS  $I_{\text{fix}}(\omega)$  is calculated from the spectral distribution of eigenfrequencies  $\omega$ .

We replace the second term of Eq. (3) by  $\Delta I(\omega)$  defined by

$$\Delta I(\omega) = \frac{L^2}{4\pi} \omega^2 - I_{\text{fix}}(\omega). \quad (7)$$

The difference  $\Delta I(\omega)$  for a square drum with  $L=1999$  (namely,  $n=2000$ ) is calculated by putting the rigorous result for  $I_{\text{fix}}(\omega)$  into Eq. (7). The data (a) in Fig. 1 show the frequency dependence of  $\Delta I(\omega)$  obtained using Eq. (7). The difference  $\Delta I(\omega)$  is not proportional to  $\omega$  in the frequency regime higher than  $\omega \approx 0.1$ . This indicates that the IDOS for the discretized drum under the stress-free boundary condition is not expressed by the first term  $L^2\omega^2/4\pi$  of Eq. (7) in this high frequency regime. This arises from the fact that our drum possesses a finite grid spacing  $a$ . Thus the IDOS for the discretized drum obeys the WSP conjecture [Eq. (3)] only in a very narrow frequency region.

The first term of Eq. (3) represents the IDOS for a continuum drum with the stress-free boundary. Therefore, we replace the first term of Eq. (7) by the IDOS  $I_{\text{free}}(\omega)$  for a discretized system with the stress-free boundary,

$$\Delta I(\omega) = I_{\text{free}}(\omega) - I_{\text{fix}}(\omega). \quad (8)$$

In the case of the discretized square drum with the stress-free boundary, the dispersion relation becomes the same with Eq. (5), but the wave numbers are expressed by

$$k'_\alpha = \frac{p'\pi}{n-2}; \quad \text{for } p'=0,1,2,\dots,n-1. \quad (9)$$

Equations (5), (6), and (9) lead the rigorous form of the difference  $\Delta I(\omega)$  of Eq. (8) for the discretized square drum. The result is shown by the data (b) in Fig. 1. This shows clearly that  $\Delta I(\omega)$  is proportional to  $\omega$  even in the higher frequency regime (over two orders of frequency range) compared with the case of the data (a). Thus we can properly replace the first term of the WSP asymptotic formula (3) with the IDOS  $I_{\text{free}}(\omega)$  of the discretized system. Extending this idea, we claim the following relation to be the discretized version of the BL conjecture,

$$I_{\text{fix}}(\omega) = I_{\text{free}}(\omega) - B_f \omega^{D_f}. \quad (10)$$

#### IV. OUTLINE OF NUMERICAL METHOD

The method employed for calculations of the densities of states (DOS) and eigenmodes is the forced oscillator method (FOM) [20–23]. This method is based on the principle that a linear dynamical system driven by a periodic external force

of frequency  $\Omega$  will respond with large amplitudes in those eigenmodes close to this frequency. This method enables us to calculate in an efficient way the spectral density of states, eigenvalues, and their eigenvectors of very large Hermitian [20,21] or non-Hermitian matrices [22]. The algorithm can treat a system with a size of the order of  $N=10^7$  using a computer with 1 Gbyte memory space. Such a large size makes it possible to obtain correct insight into the spectral densities of states of fractal drums.

Let us introduce the Lagrangian of a classical vibrational system with unit mass of the form,

$$L = \frac{1}{2} \sum_m \dot{u}_m^2 - \frac{1}{2} \sum_{mn} D_{mn} u_m u_n + \sum_m F_m u_m \cos(\Omega t), \quad (11)$$

where  $m$  (and  $n$ ) represents the grid point on the 2D drum.  $u_m$  denotes the scalar displacement of the  $m$ th site and  $D_{mn}$  is the spring constant (the matrix element) between the  $m$ th and  $n$ th site. The coefficient  $F_m$  is the amplitude of the external force applied to the  $m$ th site, and  $\Omega$  is the driving frequency. The first and second terms in Eq. (11) are the kinetic energy and the potential energy of coupled harmonic oscillators, respectively, and the third represents the external field. Varying the frequency  $\Omega$ , the density of states in an arbitrary range is calculated as follows [20–23].

The Lagrangian Eq. (11) without the external field yields the lattice dynamical equation of motion of the form

$$\frac{d^2}{dt^2} u_m(t) = - \sum_n D_{mn} u_n(t). \quad (12)$$

By discretizing time  $t$  into steps  $\tau$ , Eq. (12) becomes coupled equations,

$$\begin{aligned} v_m(i+1) &= v_m(i) - \tau \sum_n D_{mn} u_n(i), \\ u_m(i+1) &= u_m(i) + \tau v_m(i+1), \end{aligned} \quad (13)$$

where  $v_m(i)$  is the velocity of the  $m$ th particle at time  $t=i\tau$  where the integer  $i$  denotes the time in units of  $\tau$  [20]. Each displacement  $u_m(i)$  and velocity  $v_m(i)$  can be decomposed into a sum of normal modes  $e_m(\lambda)$  as

$$\begin{aligned} u_m(i) &= \sum_\lambda Q_\lambda(i) e_m(\lambda), \\ v_m(i) &= \sum_\lambda P_\lambda(i) e_m(\lambda), \end{aligned} \quad (14)$$

where  $Q_\lambda(i)$  and  $P_\lambda(i)$  are the time-dependent amplitudes with which the mode  $\lambda$  contributes to  $u_m(i)$  and  $v_m(i)$ , respectively, and vary as  $\exp(-i\omega_\lambda t)$  as seen from substituting Eq. (14) into (12). The displacement  $u_m(i)$  is set to be zero at  $i=0$ , then the periodic forces  $F_m \cos(\Omega \tau i)$  are imposed on each site  $m$  in Eq. (13). Here  $F_m$  is chosen as  $F_m = F_0 \cos(\phi_m)$ , where  $\phi_m$  is a random quantity taking a value within the range  $0 \leq \phi_m < 2\pi$ , and  $F_0$  is a constant.

As a next step, we define the energy  $E(i)$  given by

$$\begin{aligned}
E(i) &= \frac{1}{2} \left\{ \sum_m [v_m(i)]^2 + \sum_m \sum_n u_m(i) D_{mn} u_n(i) \right\} \\
&= \frac{1}{2} \sum_\lambda |\xi_\lambda(i)|^2,
\end{aligned} \tag{15}$$

where the orthogonality condition between eigenvectors is used. We have introduced the quantity  $\xi_\lambda(i)$  defined by  $\xi_\lambda(i) \equiv Q_\lambda(i) + i\omega_\lambda Q_\lambda(i)$ . After a sufficiently large time-interval  $T$ ,  $\xi_\lambda(i)$  becomes from Eqs. (12) and (14),

$$\xi_\lambda(T) \approx \frac{e^{i\omega_\lambda T}}{2} \left\{ \sum_m F_m e_m(\lambda) \right\} \frac{e^{i(\Omega - \omega_\lambda)T} - 1}{i(\Omega - \omega_\lambda)}. \tag{16}$$

Using Eqs. (15) and (16), one has the energy gained by the external force as,

$$E(T) = \frac{1}{2} \sum_\lambda \left\{ \sum_m F_m e_m(\lambda) \right\}^2 \frac{\sin^2\{(\omega_\lambda - \Omega)T/2\}}{(\omega_\lambda - \Omega)^2}. \tag{17}$$

The averaged value of  $E(T)$  over the random variables  $\phi_m$  becomes

$$\begin{aligned}
\langle E(T) \rangle &= \frac{F_0^2}{2} \sum_\lambda \frac{\sin^2\{(\omega_\lambda - \Omega)T/2\}}{(\omega_\lambda - \Omega)^2} \\
&\quad \times \left\langle \sum_m \sum_n e_m(\lambda) e_n(\lambda) \cos(\phi_m) \cos(\phi_n) \right\rangle \\
&= \frac{F_0^2}{4} \sum_\lambda \frac{\sin^2\{(\omega_\lambda - \Omega)T/2\}}{(\omega_\lambda - \Omega)^2},
\end{aligned} \tag{18}$$

where  $\langle \dots \rangle$  represents the random phase average and the terms satisfying  $m=n$  remain in the summations with respect to  $m$  and  $n$ . For sufficiently large  $T$ , only the modes belonging to eigenfrequencies  $\omega_\lambda$  within the narrow frequency range near  $\Omega$  contribute to the sum in Eq. (18).

For large system size  $N$ , it is not necessary to average over all possible ensembles  $\{\phi_m\}$  explicitly due to the self-average. Provided that the proper time-interval  $T$  is taken, Eq. (18) yields

$$\begin{aligned}
\langle E(\Omega, T) \rangle &= \frac{\pi T F_0^2}{8} \sum_\lambda \delta(\omega_\lambda - \Omega) \\
&= \frac{\pi T N F_0^2}{8} D(\Omega),
\end{aligned} \tag{19}$$

where  $D(\Omega)$  is the density of states for the mapped system. Here we have used the relation  $\lim_{T \rightarrow \infty} \sin^2(xT)/\pi T x^2 = \delta(x)$ . The resonance width  $\delta\omega$  is inversely proportional to the time  $T$ , as given by  $\delta\omega = 4\pi/T$ .

The eigenmodes  $\lambda$  are calculated by the following procedures. By applying the external force  $F_m \cos(\Omega \tau i)$  to the system, the amplitude of  $u_m(i)$  after the time-interval  $T$  can be written as, using Eqs. (12) and (14) and taking the initial condition  $P_\lambda(i=0)=0$ ,

$$\begin{aligned}
u_m(T) &= \sum_\lambda \left\{ \sum_n F_n e_n(\lambda) \right\} \\
&\quad \times \frac{2 \sin\{(\Omega + \omega_\lambda)T/2\} \sin\{(\Omega - \omega_\lambda)T/2\}}{\Omega^2 - \omega_\lambda^2} e_m(\lambda).
\end{aligned} \tag{20}$$

For sufficiently large time  $T$ , only a few eigenmodes with eigenfrequencies  $\omega_\lambda$  close to  $\Omega$  have large amplitudes. One can accelerate the calculation by replacing the amplitude of the periodic force  $F_m$  at each site  $m$  by  $F_m = u_m(T)$ . Initial amplitude  $u_m(i=0)$  at the  $m$ th site is set to be zero again, and we follow the time developments of Eq. (13) with the new external force  $F_m \cos(\Omega \tau i)$ . After  $p$  iterations of this procedure, the amplitude  $u_m(T)$  becomes

$$\begin{aligned}
u_m^{(p)}(T) &= \sum_\lambda \left\{ \sum_n F_n e_n(\lambda) \right\} \\
&\quad \times \left[ \frac{2 \sin\{(\Omega + \omega_\lambda)T/2\} \sin\{(\Omega - \omega_\lambda)T/2\}}{\Omega^2 - \omega_\lambda^2} \right]^p e_m(\lambda).
\end{aligned} \tag{21}$$

For sufficiently large  $p$ , only a single eigenmode  $\lambda_1(\omega_{\lambda_1} \approx \Omega)$  survives such as

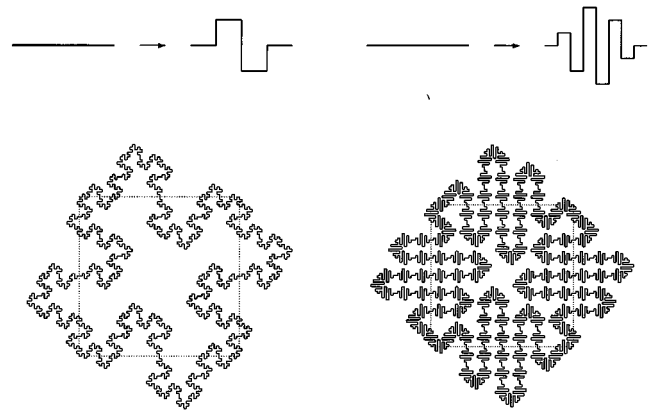
$$u_m^{(p)}(T) \approx C e_m(\lambda_1), \tag{22}$$

where  $C$  is a constant.

The formula for judging the accuracy of calculated eigenvectors has been given in Ref. [21]. The key quantity is

$$\delta^2(\mu) \equiv \frac{\sum_m \{a_m - \mu^2 u_m^{(p)}(T)\}^2}{\sum_m a_m^2}, \tag{23}$$

where  $\mu$  is a parameter and  $a_m \equiv \sum_n D_{mn} u_n^{(p)}(T)$ . It is evident that, if only a single mode  $\lambda_1$  is excited, the value of



(a) The fractal drum A with  $D_f = 3/2$

(b) The fractal drum B with  $D_f = 5/3$

FIG. 2. Illustrations of fractal drums. Each generator is given above. (a) The fractal drum with the Koch-curve perimeter at the third generation  $\nu=3$ . The fractal dimension of the Koch-curve is  $D_f = \ln 8 / \ln 4 = 3/2$ . (b) The fractal drum with  $D_f = \ln 32 / \ln 8 = 5/3$ . The dotted lines shown in (a) and (b) indicate the initiators (square drum).

TABLE I. Parameters used in our numerical simulations. Drums A and B are illustrated in Figs. 2(a) and (b), respectively. Drum C is the Koch drum at the first generation  $\nu=1$ , which is employed for calculating the localized edge mode.

	drum A	drum B	drum C
$D_f$	3/2	5/3	3/2
$\nu$	3	2	1
$l$	29a	24a	49a
$L$	3074a	2832a	294a
$N$	3 474 433	2 408 449	39 201
$N_p$	59 392	98 304	1568
$N_p/N$	0.0171	0.0408	0.0400

$\delta^2(\omega_{\lambda_1})$  becomes zero. When the excited pattern consists of a few modes with eigenfrequencies close to the mode  $\omega_{\lambda_1}$ ,  $\delta$  becomes small when the frequency  $\mu$  is close to  $\omega_{\lambda_1}$ . Therefore  $\delta(\mu)$  gives an index for the degree of accuracy.

We should stress the following advantages to compute the DOS in terms of the FOM: (i) Calculations can be performed within an arbitrary energy range one needs, (ii) the energy

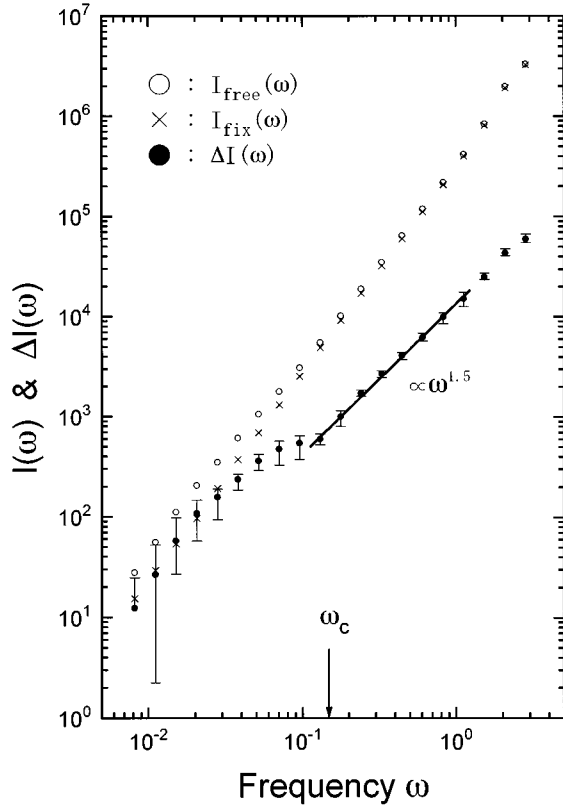


FIG. 3. The IDOS's  $I_{\text{free}}(\omega)$  and  $I_{\text{fix}}(\omega)$ , for the drum A as a function of frequency  $\omega$  with error bars. We use the system of units  $m=1$ ,  $K=1$ , and  $a=1$ . The results show the averaged IDOS's over four sets of  $\{\phi_m\}$ . Open circles and crosses indicate the IDOS's of drums with the free (Neumann) and fixed (Dirichlet) boundary conditions, respectively. Filled circles indicate the difference  $\Delta I(\omega)$  which is proportional to  $\omega^{1.5}$  ( $=\omega^{D_f}$ ) in the frequency regime higher than a characteristic frequency  $\omega_c$ . In the frequency regime lower than  $\omega_c$ ,  $\Delta I(\omega)$  does not follow the power-law dependence  $\omega^{D_f}$ .

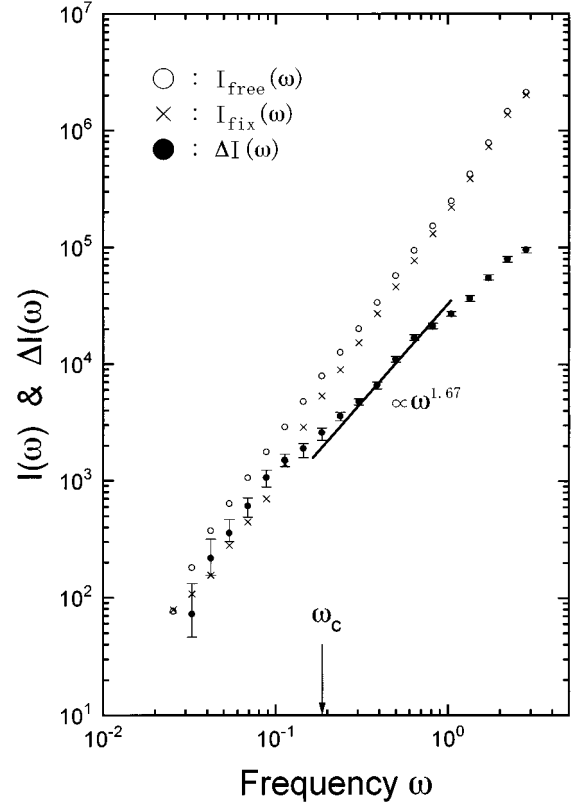


FIG. 4. The IDOS's  $I_{\text{free}}(\omega)$  and  $I_{\text{fix}}(\omega)$ , for the fractal drum B as a function of frequency  $\omega$  with error bars, where  $m=1$ ,  $K=1$ , and  $a=1$ . The results show the averaged IDOS's over six sets of  $\{\phi_m\}$ . The definitions of symbols are the same with those given in Fig. 3. The difference  $\Delta I(\omega)$  is proportional to  $\omega^{1.67}$  in the frequency regime higher than a characteristic frequency  $\omega_c$ .

resolution can be controlled by taking the appropriate time-interval  $T$ , (iii) the CPU time is proportional to the system size  $N$ , and (iv) the accuracy of the calculated DOS increases with increasing the system size  $N$ .

## V. NUMERICAL RESULTS

We have computed the IDOS's of two different Koch drums as illustrated in Figs. 2(a) and (b). The fractal dimensions of boundaries in Figs. 2(a) and (b) are  $D_f=3/2$  and  $D_f=5/3$ , respectively. The index  $\nu$  indicates the generation of the fractal boundary, where the total length of perimeter increases with the generation. The symbols  $l$  and  $L$  show the lengths of the segment at the fractal boundary and the system size, respectively. The length  $l$  is taken to be larger than the grid spacing  $a$ , namely, we have chosen the values of  $l$  as  $l=29a$  and  $24a$  for the drums A [Fig. 2(a)] and B [Fig. 2(b)], respectively. These fractal drums consist of the grid points of  $N$  including  $N_p$  sites on the perimeter. Table I gives the parameters used in our computations.

The difference  $\Delta I(\omega)$  has been calculated from both  $I_{\text{free}}(\omega)$  and  $I_{\text{fix}}(\omega)$  by using the formula Eq. (8). The resonance width  $\delta\omega=4\pi/T$  is taken to be proportional to the frequency  $\omega$ , namely, the time-interval  $T$  for our simulations is taken as

$$T = \frac{4\pi}{\delta\omega} = \frac{16\pi}{\omega}. \quad (24)$$

This choice enables us to have a constant frequency resolution of the DOS when plotting the data in a log-log scale. We have taken the sample average of four to six sets of random variables  $\{\phi_m\}$ .

### A. Integrated density of states

The dispersion relation of a lattice system deviates significantly from the linear law in the high frequency region. Due to this reason, we evaluate the IDOS in the frequency regime  $\omega \lesssim 1.0$  as argued in Sec. III. Figure 3 shows our numerical results on the frequency dependence of the IDOS for the drum A with the fractal dimension  $D_f = 3/2 = 1.5$  [Fig. 2(a)], where the average is taken over four sets of  $\{\phi_m\}$ . Open circles and crosses indicate the IDOS's of drums with free and fixed boundary conditions, respectively. Filled circles with error bars are the results for the difference  $\Delta I(\omega)$  computed from Eq. (8). Figure 3 gives clear evidence that the difference  $\Delta I(\omega)$  is proportional to  $\omega^{1.5}$  in the frequency regime higher than a characteristic frequency  $\omega_c$ . Hereafter, we call vibrational modes of a drum with the fixed boundary ‘‘bulk modes’’ and modes in the boundary region ‘‘edge modes.’’ The total number of edge modes is small compared with that of bulk modes. In fact, the degree of freedom of the perimeter ( $N_p$ ) is a few percent of that of the whole drum ( $N$ ) in our calculations (see Table I).

The physical implication on the characteristic frequency  $\omega_c$  can be given by comparing the length scale of the wavelength  $\lambda$  and the segment length  $l$  at the perimeter as follows: The BL conjecture is based on the assumption that vibrations of a drum with the stress-free boundary can be separated into the bulk and the edge modes. In addition, the assumption of the linear dispersion relation for the edge modes is not appropriate. This implies that the BL conjecture is not valid in the low frequency region such as  $\lambda/l \gg 1$ . We claim that the characteristic frequency  $\omega_c$  is related to the excited mode

with the wavelength  $\lambda \approx 2l$ . Since  $l = 29a$  for the drum A,  $\omega_c$  of this drum should become 0.153 which is calculated from the dispersion relation. This value agrees quite well with the characteristic frequency  $\omega_c$  obtained in Fig. 3, which indicates, contrary to Ref. [7] that Eq. (10) holds when the wavelengths  $\lambda$  of vibrational excitations of a fractal drum are shorter than the length scale  $l$  characterizing the fractal perimeter.

We have also computed the IDOS of the drum B with the different fractal perimeter [see Fig. 2(b)], for which the fractal dimension of the boundary is  $D_f = 5/3 \approx 1.67$ . In order to obtain high enough accuracy of the DOS, the time-interval  $T$  is taken as  $T = 4\pi/\delta\omega = 30\pi/\omega$ . The calculated results are shown in Fig. 4, where the average is taken over six sets of random variables  $\{\phi_m\}$ . The definitions of symbols in Fig. 4 are the same with those given in Fig. 3. Since the length of the fractal segment  $l$  is taken to be  $24a$  (see Table I), the characteristic frequency  $\omega_c$  should become 0.185. This coincides with the calculated value indicated in Fig. 4. The result shows that  $\Delta I(\omega)$  is proportional to  $\omega^{1.67}$  in the high frequency region  $\omega > \omega_c$ . In the lower frequency regime than  $\omega_c$ ,  $\Delta I(\omega)$  does not follow the power-law dependence  $\omega^{1.67}$ . The important feature of the calculated results in Fig. 4 is the oscillating behavior of the  $\Delta I(\omega)$   $\omega_c$ . This feature is also observed for the case of the drum A as shown in Fig. 3. This point will be argued later.

### B. Mode patterns

We have demonstrated that Eq. (10) holds under the condition that the wavelengths  $\lambda$  of vibrational excitations are shorter than the length scale  $l$  characterizing the fractal perimeter. We have computed mode patterns localized near the fractal boundary of a fractal drum with the stress-free boundary. These provide one of evidences supporting the validity of the BL conjecture.

The method employed for calculating mode patterns is the forced oscillator method [20–23] mentioned in Sec. III. We use a Koch drum at the first generation with the stress-free

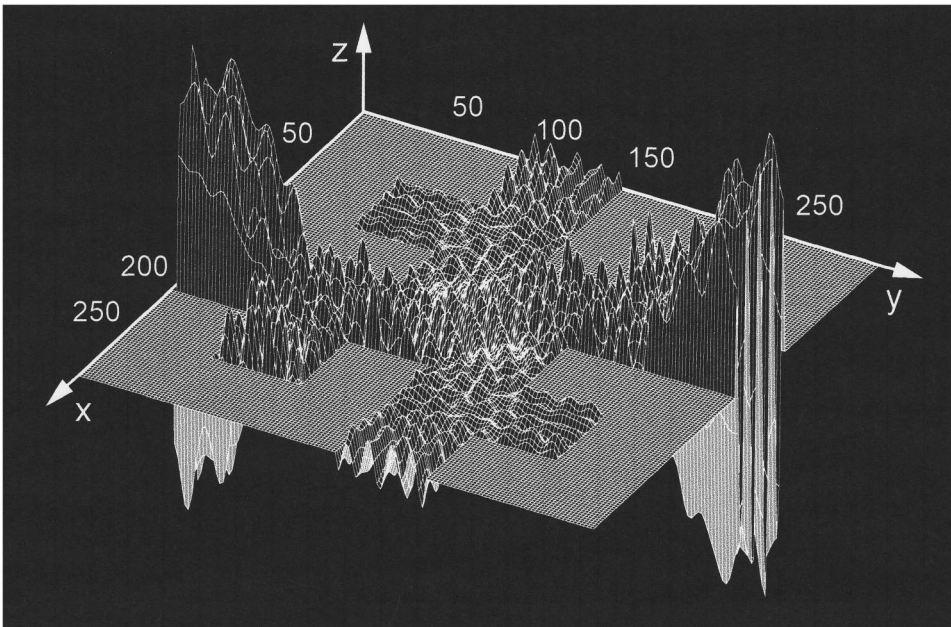


FIG. 5. The eigenmode with the eigenfrequency  $\omega = 0.498\ 068\ 61$  for the Koch drum ( $\nu = 1$ ) with the stress-free boundary condition. Large amplitudes are observed at both ends of the drum.

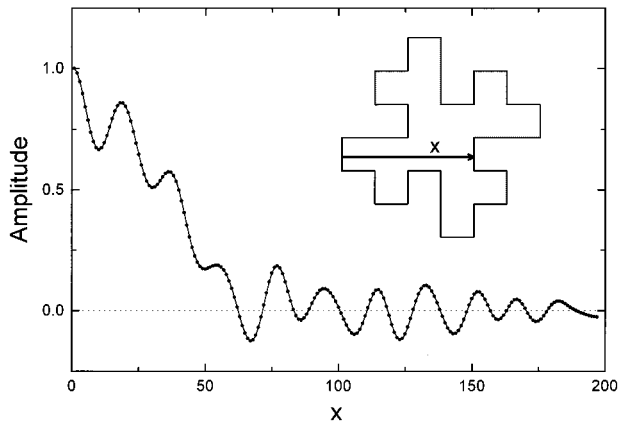


FIG. 6. Cross section of the mode pattern along the  $x$  axis given in the inset. For the region  $1 \leq x \leq 50$ , the amplitudes are very large.

boundary condition. The parameters of the drum are  $l=49a$ ,  $L=294a$ ,  $N=39\,201$ , and  $N_p=1\,568$  (see Table I). We choose the large number of grid points at the perimeter such as  $l=49a$ , in order to clarify the characteristics of eigenmodes. Using these values of parameters and the dispersion relation, the characteristic frequency  $\omega_c$  of the Koch drum is estimated to be 0.09. The calculated result is shown in Fig. 5, where the mode pattern with the eigenfrequency  $\omega=0.498\,068\,61$  is presented. The value of the quantity  $\delta(\mu)$  introduced in Eq. (23) for the judgement of the purity of the eigenmode is  $0.85 \times 10^{-6}$ . Figure 5 shows that the mode vibrates with large amplitudes at both ends of the drum with antiphase. The displacements near the boundary are larger than those in other regions, and the displacements decrease toward the inside of the drum. We have plotted the amplitude of this mode in Fig. 6, where a cross section along the  $x$  axis defined in the inset is given. For  $1 \leq x \leq 50$ , the amplitudes are large compared with those in the region  $x \geq 50$ . It should be noted that the mode vibrates sinusoidally along the  $y$  axis. These edge modes are not extended along the perimeter. This feature is in contrast to the case of a drum with the smooth boundary, where edge modes are extended along the perimeter.

## VI. SUMMARY AND DISCUSSIONS

We have investigated vibrational characteristics of drums with self-similar boundaries via large-scale simulations, paying attention to the BL conjecture on the spectral distribu-

tion. The applicability of the conjecture for discretized systems has been argued in detail. We have used the formula Eq. (10) for discretized drums instead of the conjecture Eq. (4) for continuum media. We have demonstrated the validity of the formula (10) proposed in the present paper for the case of a square drum with the smooth perimeter, i.e., the calculated IDOS coincides fairly well with the WSP asymptotic formula (3). The IDOS's of fractal drums with the fractal dimensions of the perimeters  $D_f=3/2$  and  $D_f=5/3$  have been computed. The results show that  $I_{\text{fix}}(\omega)$  obeys Eq. (10) in the frequency regime higher than  $\omega_c$ , where  $\omega_c$  is related to the length scale  $l$  characterizing the fractal perimeter. The criterion for the validity of Eq. (10) has become clear, namely, the conjecture holds for modes with wavelengths  $\lambda$  shorter than the length scale  $l$  characterizing the fractality of the perimeter. Figure 5 gives eigenmode localized at the fractal (stress-free) boundary of the Koch drum ( $\nu=1$ ) with the fractal dimension  $D_f=3/2$  of the perimeter.

Recently, Levitin and Vassiliev [18] and Fleckinger, Levitin, and Vassiliev [19] have pointed out that the BL conjecture Eq. (4) for fractal drums is not rigorous. They have suggested [18,19] that the coefficient  $B_f$  in Eqs. (4) and (10) is an oscillating function of frequency  $\omega$ , but the amplitude is very small. We have tried to reveal this behavior. The oscillation with small amplitudes has been observed as shown in Figs. 3 and 4 within our numerical accuracy. The problem suggested by Levitin and co-workers [18,19] will be crucial for further development on the present subject.

Our results are applicable to various fields of physics due to the generality of Eq. (1). One example concerns with electronic states in tailor-made mesoscopic systems with fractal perimeters [24,25]. Advances in nanostructure technology make possible the manufacture of such mesoscopic systems. Electrons confined in a 2D small region will be severely affected by the shape of the perimeter [26]. Studies on fractal drums will give an insight into electronic properties of mesoscopic systems.

## ACKNOWLEDGMENTS

This work was supported in part by a Grant-in-Aid for Scientific Research on the Special Project, "Cooperative Phenomena in Complex Liquids," from the Japan Ministry of Education, Science, and Culture (MESC). We thank Dr. M. Levitin for helpful information concerning their recent works.

[1] See, for example, B. B. Mandelbrot, *The Fractal Geometry of Nature* (Freeman, San Francisco, 1982).  
 [2] See, for example, J. Feder, *FRACTALS* (Plenum, New York, 1988).  
 [3] See, for example, D. Stauffer and A. Aharony, *Introduction to Percolation Theory* (Taylor and Francis, London, 1992).  
 [4] T. Nakayama, K. Yakubo, and R. Orbach, *Rev. Mod. Phys.* **66**, 381 (1994).  
 [5] S. Alexander and R. Orbach, *J. Phys. (Paris) Lett.* **43**, L625 (1982).

[6] B. Sapoval, Th. Gobron, and A. Margolina, *Phys. Rev. Lett.* **67**, 2974 (1991).  
 [7] M. V. Berry, in *Structural Stability in Physics*, edited by W. Guttinger and H. Elkeimer (Springer-Verlag, Berlin, 1979), pp. 51–53.  
 [8] M. L. Lapidus, *Trans. Am. Math. Soc.* **325**, 465 (1991), and references therein.  
 [9] M. L. Lapidus, in *Ordinary and Partial Differential Equations*, Vol. IV, Pitman Research Notes in Mathematics Series 289 (Pitman, New York, 1993); *Proceedings of the Twelfth Dundee*

- International Conference on the Theory of Ordinary and Partial Differential Equations*, edited by B. D. Sleeman and R. J. Jarvis (Longman Scientific and Technical, London, 1993), pp. 126–209.
- [10] M. L. Lapidus, IFIP Trans. A, Comput. Sci. Technol. (Netherlands) **A-41**, 255 (1994).
- [11] B. Sapoval, Physica D **38**, 296 (1989).
- [12] B. Sapoval, Physica A **191**, 321 (1992).
- [13] B. Sapoval and Th. Gobron, Phys. Rev. E **47**, 3013 (1993).
- [14] Y. Hobiki, K. Yakubo, and T. Nakayama, Phys. Rev. E **52**, R1310 (1995).
- [15] H. Weyl, Math. Ann. **71**, 441 (1912).
- [16] R. T. Seeley, Adv. Math. **29**, 244 (1978); R. T. Seeley, Am. J. Math. **102**, 869 (1980).
- [17] T. L. Pham, Math. Scand. **48**, 5 (1981).
- [18] M. Levitin and D. Vassiliev, Proc. London Math. Soc. **72**, 178 (1996).
- [19] J. Fleckinger, M. Levitin, and D. Vassiliev, Proc. London Math. Soc. **71**, 372 (1995).
- [20] M. L. Williams and H. J. Maris, Phys. Rev. B **31**, 4508 (1985).
- [21] K. Yakubo, T. Nakayama, and H. J. Maris, J. Phys. Soc. Jpn. **60**, 3249 (1991).
- [22] T. Terao, K. Yakubo, and T. Nakayama, Phys. Rev. E **50**, 566 (1994).
- [23] See, also a review, T. Nakayama, *Computational Physics as a New Frontier in Condensed Matter Research*, edited by H. Takayama *et al.* (The Physical Society of Japan, Tokyo, 1995), pp. 21–33.
- [24] H. Bruus and A. D. Stone, Phys. Rev. B **50**, 18275 (1994).
- [25] E. R. Mucciolo, V. N. Prigodin, and B. L. Altshuler, Phys. Rev. B **51**, 1714 (1995).
- [26] See, for example, R. E. Prange, E. Ott, T. M. Antonsen, Jr., B. Georgeot, and R. Blümel, Phys. Rev. E **53**, 207 (1996).